



Synthesis of $\text{Mn}_x\text{Ga}_{1-x}\text{Fe}_2\text{O}_4$ magnetic nanoparticles by thermal decomposition method for medical diagnosis applications



Javier Sánchez^{a,*}, Dora Alicia Cortés-Hernández^a, José Concepción Escobedo-Bocardo^a, José Manuel Almanza-Robles^a, Pamela Yajaira Reyes-Rodríguez^a, Rosario Argentina Jasso-Terán^a, Pascual Bartolo-Pérez^b, Laura Elena De-León-Prado^a

^a CINVESTAV-IPN, Unidad Saltillo, Industria Metalúrgica 1062, Parque Industrial Saltillo – Ramos Arizpe, Ramos Arizpe, Coahuila CP 25900, México

^b CINVESTAV-IPN, Unidad Mérida, Departamento de Física Aplicada, A. P. 73 Cordemex, 97310 Mérida, Yuc., México

ARTICLE INFO

Keywords:

Thermal decomposition
Magnetic nanoparticles
Medical diagnosis
Gallium ferrite

ABSTRACT

In this work, the synthesis of $\text{Mn}_x\text{Ga}_{1-x}\text{Fe}_2\text{O}_4$ ($x=0-1$) nanosized particles by thermal decomposition method, using tetraethylene glycol (TEG) as a reaction medium, has been performed. The crystalline structure of the inverse spinel obtained in all the cases was identified by X-ray diffraction (XRD). Vibration sample magnetometry (VSM) was used to evaluate the magnetic properties of ferrites and to demonstrate their superparamagnetic behavior and the increase of magnetization values due to the Mn^{2+} ions incorporation into the FeGa_2O_4 structure. Transmission electron microscopy, energy dispersive spectroscopy (TEM-EDS) and X-ray photoelectron spectroscopy (XPS) were used to characterize the obtained magnetic nanoparticles (MNPs). These MNPs showed a near spherical morphology, an average particle size of 5.6 ± 1.5 nm and a TEG coating layer on their surface. In all the cases MNPs showed no response when submitted to an alternating magnetic field (AMF, 10.2 kA/m, 354 kHz) using magnetic induction tests. These results suggest that the synthesized nanoparticles can be potential candidates for their use in biomedical areas.

1. Introduction

Magnetic nanoparticles (MNPs) of iron oxide possessing a superparamagnetic behavior are ideal materials for their use in biomedical applications such as hyperthermia thermoseeds [1–4], contrast agents for MRI diagnosis [5–9], targeted drug delivery [10–13], cell separation, biosensors [14–16], etc. Thermal decomposition of metallic organic precursors at low temperatures (≤ 350 °C) is an efficient method used for MNPs synthesis with a nanometric size and a superparamagnetic behavior. In addition, the uncontrolled aggregation among them is decreased due to the deposition of a coating on MNPs during the synthesis process. This method has been used to synthesize several types of magnetic oxides such as Fe_3O_4 [17,18], MnFe_2O_4 [19,20], CoFe_2O_4 [21,22], $\text{MnZnFe}_2\text{O}_4$ [23], ZnFe_2O_4 [24] for their potential application in biomedical areas.

On the other hand, it has been reported that gallium can be used for the treatment of different kinds of diseases such as cancer and hypercalcemia [25], while manganese is required for many important ubiquitous enzymatic reactions [26], when these elements are present into the human body as ionic species. Based on the above mentioned properties of Ga and Mn elements and the known magnetic behavior of

Mn and Fe ions, in this work the synthesis of $\text{Mn}_x\text{Ga}_{1-x}\text{Fe}_2\text{O}_4$ ($x=0-1$) magnetic nanoparticles by thermal decomposition method is presented, evaluating the effect of Mn ions incorporation on the magnetic properties and heating ability of the synthesized samples.

2. Materials and methods

Iron III acetylacetonate ($\text{C}_{15}\text{H}_{21}\text{FeO}_6$), gallium III acetylacetonate ($\text{C}_{15}\text{H}_{21}\text{GaO}_6$), manganese II acetylacetonate ($\text{C}_{15}\text{H}_{21}\text{MnO}_6$) and tetraethyleneglycol (TEG) were used for the synthesis of MNPs. Stoichiometric amounts of the organic precursors at a ratio 2:1 of Fe:Ga-Mn were placed into a three-necked flask that already contained 40 mL of TEG as reaction medium. The mixture was ultrasonically stirred during 15 min to obtain a homogenous precursor solution. The three-necked flask was then adapted to a reflux condenser system and heated at 250 °C for 60 min with the aim to promote the decomposition of organic precursor into CO_2 and water and the formation of the crystalline structure. The synthesized material was washed with ethanol and dried in a stove at 95 °C for their physicochemical characterization. Powders identification and the lattice parameter (a) calculation, taking into account the Miller indices (hkl) and the

* Corresponding author.

E-mail address: h_javiersanchez@hotmail.com (J. Sánchez).

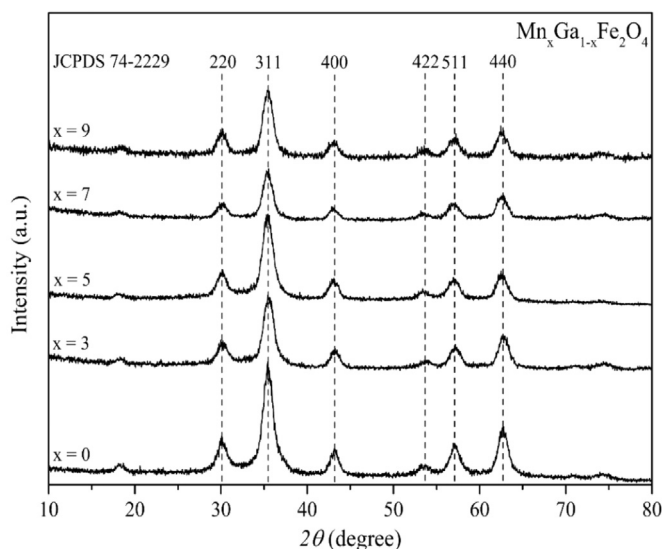


Fig. 1. XRD patterns of $Mn_xGa_{1-x}Fe_2O_4$ ($x=0, 0.3, 0.5, 0.7$ and 0.9 of Mn^{2+}) synthesized samples.

Table 1
Magnetic properties, cell parameter and crystallite size of $Mn_xGa_{1-x}Fe_2O_4$ ($x=0-1$).

Sample	M_s (emu/ g)	M_r (emu/ g)	H_c (Oe)	Crystallite size (nm)	Lattice parameter (a), (Å)
$FeGa_2O_4$	22.8	0.045	2.610	6	8.3913
$Mn_{0.1}Ga_{0.9}Fe_2O_4$	48.2	0.007	0.186	7	8.3688
$Mn_{0.2}Ga_{0.8}Fe_2O_4$	33.4	0.013	0.562	6	8.3857
$Mn_{0.3}Ga_{0.7}Fe_2O_4$	36.3	0.378	12.06	6	8.3913
$Mn_{0.4}Ga_{0.6}Fe_2O_4$	36.5	0.002	0.097	6	8.3857
$Mn_{0.5}Ga_{0.5}Fe_2O_4$	28.4	0.209	10.38	6	8.3913
$Mn_{0.6}Ga_{0.4}Fe_2O_4$	33.1	0.008	0.344	7	8.4030
$Mn_{0.7}Ga_{0.3}Fe_2O_4$	44.9	0.065	1.830	6	8.3744
$Mn_{0.8}Ga_{0.2}Fe_2O_4$	50.5	0.004	0.142	7	8.3572
$Mn_{0.9}Ga_{0.1}Fe_2O_4$	32.6	0.006	0.278	6	8.3913
$MnFe_2O_4$	36.7	0.603	13.42	8	8.4374

interplanar distance (d) [27], was performed by XRD. For all synthesized samples, the crystallite size was calculated by the Scherrer equation [28] and the evaluation of magnetic properties was carried out by VSM technique at a constant magnetic field intensity of 12 kOe at room temperature. Selected samples ($x=0.4$ and 0.6) were characterized by XPS and TEM-EDS, which allowed the determination of size, morphology and chemical composition of powders. By solid state magnetic induction, the heating capacity of aqueous suspensions of 3.0, 4.5, 6.0 and 10.0 mg of $Mn_{0.4}Ga_{0.6}Fe_2O_4$ and $Mn_{0.6}Ga_{0.4}Fe_2O_4$ nanoparticles per mL of deionized water was tested at a constant AC magnetic field (10.2 kA/m, 354 kHz).

3. Results and discussions

In Fig. 1 the XRD patterns of selected synthesized samples are presented. In these results a slight displacement of reflections was observed in some hkl planes at high quantities of proposed cationic substitution. The powders were identified as crystalline materials and the JCPDS 74–2229 card ($FeGa_2O_4$) was used for the identification of the sample with no Mn^{2+} ($x=0$) and that of the resulting crystalline structures. All samples possess an inverse spinel structure and the calculated lattice parameter (a , Table 1) has a slight variation with the successive substitution due to the lattice expansion that took place by the ionic exchange between ions with different radiuses. Lattice parameter (a) shows either an increase or a decrease in comparison to that of $FeGa_2O_4$ (8.363 Å) and $MnFe_2O_4$ (8.515 Å), when Ga ions are

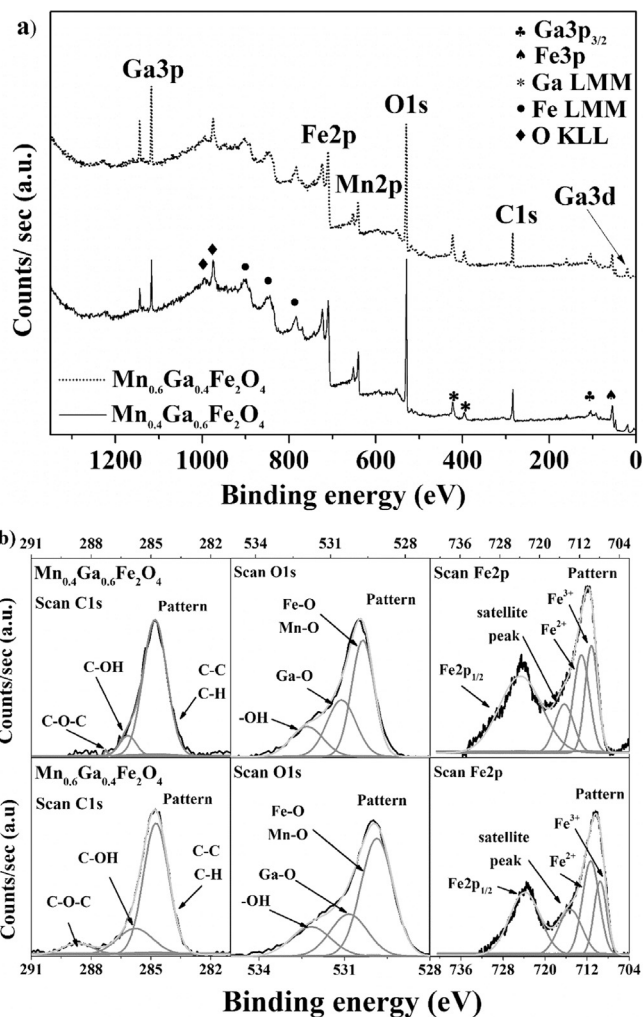


Fig. 2. XPS characterization (a) and C1s, O1s and Fe2p deconvolutions (b) of $Mn_xGa_{1-x}Fe_2O_4$ ($x=0.4, 0.6$) synthesized samples.

being replaced by Mn ions. As Mn and Ga ions are distributed into the spinel structure, the lattice parameter varies as a result of the different occupied tetrahedral (A) or octahedral (B) sites, mainly due to the coordination number and the environment in which ions are found [29]. For this reason, the lattice parameter shows no tendency as Ga ions are substituted by Mn ions. The shape and intensity of the identified reflections suggest that particles with a reduced diameter size were successfully synthesized, as it can be observed in Table 1, where the magnetic properties, the calculated lattice parameter (a) and the crystallite size are listed. The values of M_r and H_c are close to zero in almost all cases indicating that the synthesized samples have a superparamagnetic behavior, in which the magnetic moments inside the particles can be rotated as a result of either thermal fluctuations or the magnetic field application. This rotation implies the movement of magnetic moments from axis of easy magnetization and then, each particle behaves as a paramagnetic atom but with a giant magnetic moment due to the existence of a defined magnetic order inside the particles. Zero hysteresis values and a single domain particles with a ferromagnetic behavior are the characteristic properties of nanoparticles in a superparamagnetic state, where the particle loses its ability to store information when their size is below the critical radius [30].

Variations in the saturation values (M_s) were observed as a result of magnetic interactions through oxygen anions between iron and manganese ions positioned into both tetrahedral (A) and octahedral (B) sites of the spinel structure, where the magnetic moments of A and B sublattices have a parallel alignment [31]. When the proposed ex-

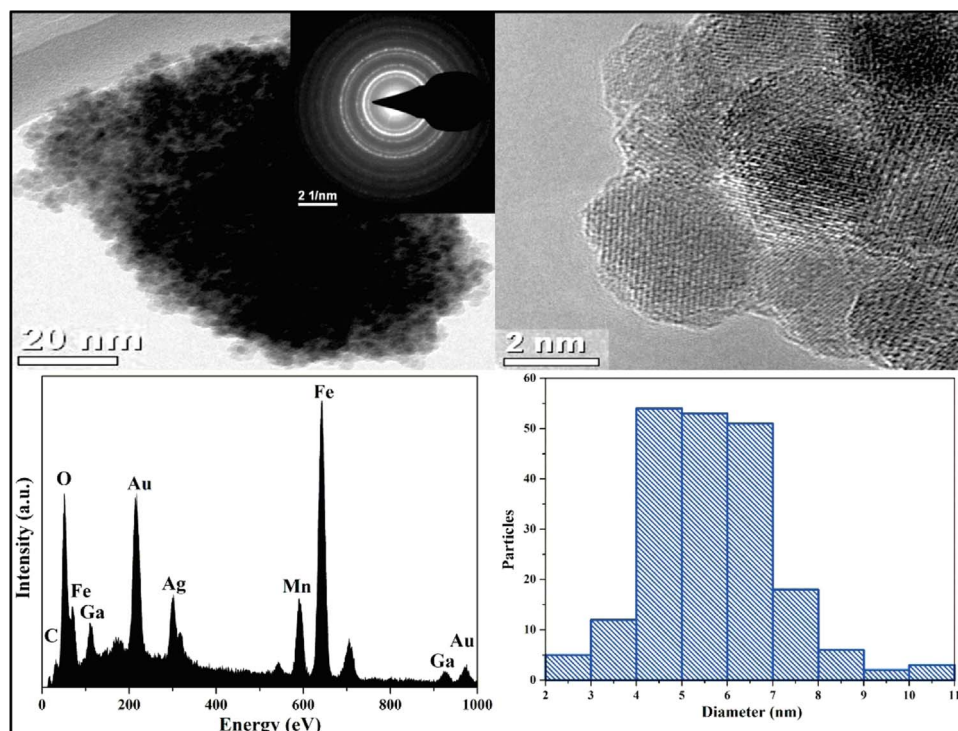


Fig. 3. TEM and SAED images, EDS spectrum and size distribution of $\text{Mn}_{0.4}\text{Ga}_{0.6}\text{Fe}_2\text{O}_4$.

change is reached it is expected that the Mn^{2+} ions can replace the Ga^{3+} ions probably located in both A and B sites, according to experimental observations of Mahmoud et al., where Mn^{2+} ions of a manganese ferrite were replaced by Ga^{3+} ions [32]. As a result of the presence of manganese with a magnetic moment of $5 \mu_{\text{B}}/\text{atom}$ [33] into both A and B sublattices, an increase of the net magnetic moment was observed, increasing M_s as compared to that corresponding to gallium ferrite (22.8 emu/g, $x=0$).

In this work, the M_s value of MnFe_2O_4 (36.7 emu/g) is lower than that reported in Dalton Trans. (46.01 emu/g) [34], which was obtained by a solothermal method using metal-oleate as the source, and similar to that reported by Yang et al. (39 emu/g) [20] for this ferrite obtained by thermal decomposition method. According to the magnetic properties of synthesized MNPs it was possible to indicate that ferrites with $x=0.4$ and 0.6 of Mn^{2+} are superparamagnetic materials for their potential use in biomedical applications.

The XPS results of analyzed MNPs are presented in Fig. 2a and the corresponding deconvolutions of C1s, O1s and Fe2p signals are shown in Fig. 2b. According to the respective binding energy of each peak, it was possible to identify the signals of Ga3d, Fe2p, Mn2p and O1s as the main elements of the magnetic oxide and the C1s signal as part of a TEG layer on the MNP's surface. The Ga-LMM, Fe-LMM and O-KLL Auger electron lines and Ga3p_{3/2} and Fe3p peaks were also identified to confirm the chemical composition of MNPs. Through the analysis of corresponding deconvolutions, it was found that the signals are composed for more than one type of bond (C1s, O1) or an oxidation state (Fe2p). For O1s signal a Ga–O bond and an overlap between Fe–O and Mn–O bonds were observed, while for C1s deconvolution two signals were identified (C–O bond and elemental C) which correspond to TEG organic molecules and finally, for Fe2p signal two different emission peaks which are chemically shifted to higher binding energies in comparison with metallic iron [35] were also detected.

Fig. 3 shows TEM and SAED images, EDS spectrum and size distribution of $\text{Mn}_{0.4}\text{Ga}_{0.6}\text{Fe}_2\text{O}_4$. As it can be observed, the particles have a near spherical morphology and the average size of the particles was calculated in 5.6 ± 1.5 nm, taking into account the log-normal distribution from the calculated values of 200 particles. This average

particle size calculated from TEM images agrees with the crystallite size calculated from XRD patterns.

A decrease of interparticle interaction was also observed, in comparison to GaFe_2O_4 MNPs synthesized by sol-gel method [36,37], reducing the Van der Waals forces and the strong magnetic attractions among particles and their possible rapid clearance by the reticuloendothelial system [38]. The EDS and SAED analysis indicate the chemical composition and the crystalline degree of samples; these agree with XPS and XRD results previously discussed. The magnetic induction results demonstrate that MNPs show no response when the AC magnetic field was applied, indicating that these MNPs possess no heating ability. This absence of heating ability may indicate that the synthesized MNPs have a size below the critical radius and thus, the anisotropy energy avoids either the magnetic moments to be relaxed at the equilibrium orientation (Néel relaxation) [39] or the rotation of particles directly inside the liquid carrier (Brownian relaxation) [40], which was not an observed behavior for sol-gel synthesized nanoparticles with the same chemical composition [37].

Taking into account that Mn-doped ferrite nanoparticles have demonstrated a higher magnetic susceptibility compared with other divalent metal dopants [41,42], the materials synthesized in this work can be potential candidates for medical diagnosis applications based on their size, superparamagnetic behavior and chemical composition of magnetic core.

4. Conclusions

Superparamagnetic nanoparticles of $\text{Mn}_x\text{Ga}_{1-x}\text{Fe}_2\text{O}_4$ ($x=0-1$) with a near spherical morphology, a nanometric size of 5.6 ± 1.5 nm and a TEG layer on MNPs surface were successfully synthesized by thermal decomposition method at 250 °C for 1 h. All synthesized samples show an increase on the saturation magnetization values (28–50 emu/g) as a result of the exchange of Ga^{3+} ions for Mn^{2+} ions into a GaFe_2O_4 ferrite, increasing the net magnetic moment between A and B sublattices of the spinel structure. Values of M_r and H_c close to zero were also observed in all synthesized samples. Magnetic induction results of $\text{Mn}_{0.4}\text{Ga}_{0.6}\text{Fe}_2\text{O}_4$ and $\text{Mn}_{0.6}\text{Ga}_{0.4}\text{Fe}_2\text{O}_4$ samples indicate that

the heating ability of nanoparticles is absent when they are submitted to an AC magnetic field. Based on these results, the selected MNPs show interesting properties for their potential application in biomedical areas.

Acknowledgements

The authors gratefully acknowledge CONACyT Mexico the Ph.D. scholarship granted to Héctor Javier Sánchez Fuentes (347034) and the research grants 222755 and 230253.

References

- [1] A. Doaga, A. Cojocariu, W. Amin, F. Heib, P. Bender, R. Hempelmann, Synthesis and characterizations of manganese ferrites for hyperthermia applications, *Mater. Chem. Phys.* 143 (2013) 305–310.
- [2] A. Iftikhar, M. Islam, M. Awan, M. Ahmad, S. Naseem, M.A. Iqbal, Synthesis of superparamagnetic particles of $Mn_{1-x}Mg_xFe_2O_4$ ferrites for hyperthermia applications, *J. Alloy. Compd.* 601 (2014) 116–119.
- [3] P. Pradhan, J. Giri, G. Samanta, H.D. Sarma, K.P. Mishra, J. Bellare, Comparative evaluation of heating ability and biocompatibility of different ferrite-based magnetic fluids for hyperthermia application, *J. Biomed. Mater. Res. B: Appl. Biomater.* 81 (2007) 2–22.
- [4] P. Pradhan, J. Giri, R. Banerjee, J. Bellare, D. Bahadur, Preparation and characterization of manganese ferrite-based magnetic liposomes for hyperthermia treatment of cancer, *J. Magn. Magn. Mater.* 311 (2007) 208–215.
- [5] U.I. Tromsdorf, N.C. Bigall, M.G. Kaul, O.T. Bruns, M.S. Nikolic, B. Mollwitz, Size and surface effects on the MRI relaxivity of manganese ferrite nanoparticle contrast agents, *Nano Lett.* 7 (2007) 2422–2427.
- [6] J. Lu, S. Ma, J. Sun, C. Xia, C. Liu, Z. Wang, Manganese ferrite nanoparticle micellar nanocomposites as MRI contrast agent for liver imaging, *Biomaterial* 30 (2009) 2919–2928.
- [7] C. Barcena, A.K. Sra, G.S. Chaubey, C. Khemtung, J.P. Liu, J. Gao, Zinc ferrite nanoparticles as MRI contrast agents, *Chem. Commun.* (2008) 2224–2226.
- [8] E.H. Kim, H.S. Lee, B.K. Kwak, B.-K. Kim, Synthesis of ferrofluid with magnetic nanoparticles by sonochemical method for MRI contrast agent, *J. Magn. Magn. Mater.* 289 (2005) 328–330.
- [9] D. Pouliquen, J. Le Jeune, R. Perdrisot, A. Ermias, P. Jallet, Iron oxide nanoparticles for use as an MRI contrast agent: pharmacokinetics and metabolism, *Magn. Reson. Imaging* 9 (1991) 275–283.
- [10] S. Rana, A. Gallo, R. Srivastava, R. Misra, On the suitability of nanocrystalline ferrites as a magnetic carrier for drug delivery: functionalization, conjugation and drug release kinetics, *Acta Biomater.* 3 (2007) 233–242.
- [11] M. Liong, J. Lu, M. Kovichich, T. Xia, S.G. Ruehm, A.E. Nel, Multifunctional inorganic nanoparticles for imaging, targeting, and drug delivery, *ACS Nano* 2 (2008) 889–896.
- [12] C. Sun, J.S. Lee, M. Zhang, Magnetic nanoparticles in MR imaging and drug delivery, *Adv. Drug Deliv. Rev.* 60 (2008) 1252–1265.
- [13] C.S. Kumar, F. Mohammad, Magnetic nanomaterials for hyperthermia-based therapy and controlled drug delivery, *Adv. Drug Deliv. Rev.* 63 (2011) 789–808.
- [14] M. Pita, J.M. Abad, C. Vaz-Dominguez, C. Briones, E. Mateo-Martí, J.A. Martín-Gago, Synthesis of cobalt ferrite core/metallic shell nanoparticles for the development of a specific PNA/DNA biosensor, *J. Colloid Interface Sci.* 321 (2008) 484–492.
- [15] J.B. Haun, T.J. Yoon, H. Lee, R. Weissleder, Magnetic nanoparticle biosensors, *Wiley Interdiscip. Rev. Nanomed. Nanobiotechnol.* 2 (2010) 291–304.
- [16] C. Jianrong, M. Yuqing, H. Nongyue, W. Xiaohua, L. Sijiao, Nanotechnology and biosensors, *Biotechnol. Adv.* 22 (2004) 505–518.
- [17] D.K. Jha, M. Shameem, A.B. Patel, A. Kostka, P. Schneider, A. Erbe, Simple synthesis of superparamagnetic magnetite nanoparticles as highly efficient contrast agent, *Mater. Lett.* 95 (2013) 186–189.
- [18] A. Roca, M. Morales, K. O'Grady, C. Serna, Structural and magnetic properties of uniform magnetite nanoparticles prepared by high temperature decomposition of organic precursors, *Nanotechnology* 17 (2006) 2783.
- [19] E. Kang, J. Park, Y. Hwang, M. Kang, J.-G. Park, T. Hyeon, Direct synthesis of highly crystalline and monodisperse manganese ferrite nanocrystals, *J. Phys. Chem. B* 108 (2004) 13932–13935.
- [20] H. Yang, C. Zhang, X. Shi, H. Hu, X. Du, Y. Fang, Water-soluble superparamagnetic manganese ferrite nanoparticles for magnetic resonance imaging, *Biomaterials* 31 (2010) 3667–3673.
- [21] A.P. Herrera, L. Polo-Corrales, E. Chavez, J. Cabarcas-Bolivar, O.N. Uwakweh, C. Rinaldi, Influence of aging time of oleate precursor on the magnetic relaxation of cobalt ferrite nanoparticles synthesized by the thermal decomposition method, *J. Magn. Magn. Mater.* 328 (2013) 41–52.
- [22] S. Gyergyek, D. Makovec, A. Kodre, I. Arçon, M. Jagodič, M. Drogenik, Influence of synthesis method on structural and magnetic properties of cobalt ferrite nanoparticles, *J. Nanopart. Res.* 12 (2010) 1263–1273.
- [23] M. Bremer, H. Langbein, W. Töpelmann, H. Scheler, Investigation on the formation of manganese-zinc ferrites by thermal decomposition of solid solution oxalates, *Thermochim. Acta* 209 (1992) 323–330.
- [24] I. Shariif, A. Zamanian, A. Behnamghader, Synthesis and characterization of $Fe_{0.6}Zn_{0.4}Fe_2O_4$ ferrite magnetic nanoclusters using simple thermal decomposition method, *J. Magn. Magn. Mater.* 412 (2016) 107–113.
- [25] J.A. Lessa, G.L. Parrilha, H. Beraldo, Gallium complexes as new promising metallodrug candidates, *Inorg. Chim. Acta* 393 (2012) 53–63.
- [26] A.W. Dobson, K.M. Erikson, M. Aschner, Manganese neurotoxicity, *Ann. N. Y. Acad. Sci.* 1012 (2004) 15–128.
- [27] B.D. Cullity, *Elements of X-ray Diffraction*, 2001.
- [28] V.K. Pecharsky, P.Y. Zavaliy, *Fundamentals of powder diffraction and structural characterization of materials*, vol. 69, 2009.
- [29] E. Pollert, *Crystal chemistry of magnetic oxides part 1: General problems – Spinel*, *Prog. Cryst. Growth Charact.* vol. 9, 1984, pp. 263–323.
- [30] D.S. Mathew, R.-S. Juang, An overview of the structure and magnetism of spinel ferrite nanoparticles and their synthesis in microemulsions, *Chem. Eng. J.* 129 (2007) 51–65.
- [31] J. Li, H. Yuan, G. Li, Y. Liu, J. Leng, Cation distribution dependence of magnetic properties of sol-gel prepared $MnFe_2O_4$ spinel ferrite nanoparticles, *J. Magn. Magn. Mater.* 322 (2010) 3396–3400.
- [32] M. Mahmoud, Low temperature Mössbauer study of gallium substitution for iron in manganese-ferrite, *Solid State Ion.* 176 (2005) 1333–1336.
- [33] P. Koirala, K. Pradhan, A.K. Kandalam, P. Jena, Electronic and magnetic properties of manganese and iron atoms decorated With BO_2 superhalogens, *J. Phys. Chem. A* 117 (2012) 1310–1318.
- [34] B. Bateer, C. Tian, Y. Qu, S. Du, Y. Yang, Z. Ren, Synthesis, size and magnetic properties of controllable $MnFe_2O_4$ nanoparticles with versatile surface functionalities, *Dalton Trans.* 43 (2014) 9885–9891.
- [35] K. Wandelt, Photoemission studies of adsorbed oxygen and oxide layers, *Surf. Sci. Rep.* 2 (1982) 1–121.
- [36] J. Sánchez, D. Cortés-Hernández, J. Escobedo-Bocardo, R. Jasso-Terán, A. Zugasti-Cruz, Bioactive magnetic nanoparticles of Fe–Ga synthesized by sol-gel for their potential use in hyperthermia treatment, *J. Mater. Sci. Mater. Med.* 25 (2014) 2237–2242.
- [37] J. Sánchez, D.A. Cortés-Hernández, J.C. Escobedo-Bocardo, J.M. Almanza-Robles, P.Y. Reyes-Rodríguez, R.A. Jasso-Terán, P. Bartolo-Pérez, L.E. De-León-Prado, Sol-gel synthesis of $Mn_xGa_{1-x}Fe_2O_4$ nanoparticles as candidates for hyperthermia treatment, *Ceram. Int* (2016).
- [38] S. Sheng-Nan, W. Chao, Z. Zan-Zan, H. Yang-Long, S.S. Venkatraman, X. Zhi-Chuan, Magnetic iron oxide nanoparticles: synthesis and surface coating techniques for biomedical applications, *Chin. Phys. B* 23 (2014) 037503.
- [39] S. Mornet, S. Vasseur, F. Grasset, P. Veverka, G. Goglio, A. Demourgues, Magnetic nanoparticle design for medical applications, *Prog. Solid State Chem.* 34 (2006) 237–247.
- [40] V. Nikiforov, Magnetic induction hyperthermia, *Russ. Phys. J.* 50 (2007) 913–924.
- [41] H. Ai, Layer-by-Layer capsules for magnetic resonance imaging and drug delivery, *Adv. Drug Deliv. Rev.* 63 (2011) 772–788.
- [42] H. Shokrollahi, Contrast agents for MRI, *Mater. Sci. Eng. C* 33 (2013) 4485–4497.